Wavelet Filtering of GNSS Network Data for the Detection and Identification of Ionospheric Disturbances Caused by Tsunamis

Yu-Ming Yang, James L. Garrison, See-Chen Lee

Purdue University

1 Problem Statement

Acoustic-Gravity Waves (AGWs) in the neutral atmosphere can induce disturbances in the ionosphere that are subsequently observable in trans-ionospheric Global Navigation Satellite System (GNSS) measurements of Total Electron Content (TEC). Disruptive events on the Earth's surface, such as earthquakes, tsunamis [1] and large explosions are known to be one source of these disturbances. Through observing the disturbances induced by a tsunami, a better capability to detect and provide warning of the imminent occurrence of the tsunami wave may be possible.

Coherent structure in the ionosphere, indicative of a propagating disturbance, can be detected by cross-correlating pairs of filtered TEC time series [2], [3]. Cross-correlating every pair of stations in a large (100's of stations) network, or sub-areas of a very large (1000's of stations) network [4] produces a greatly overdetermined system that can be inverted to estimate the horizontal components of the disturbance velocity.

Cross-correlation has a severe limitation, however, in that it assumes that only a single wave train is observable within the correlation time window. Prior studies have shown [5] that the occurrence rate of traveling ionospheric disturbances (TID's) under quiescent conditions can be quite high, with a strong seasonal dependence. Furthermore, a single event on the surface of the Earth could give rise to multiple disturbances with different arrival times [6]. It is thus quite possible that multiple disturbances could be present within the same time and space window. This could reduce the correlation magnitude, causing a disturbance to be missed, obscure the structure of the disturbance (such as multiple wave trains from different paths), or lead to incorrect estimates of the speed and direction [7]. In this paper, we investigate the use of wavelet analysis to detect these disturbances under more general conditions, and design a filter to isolate each identified wave train. Filtered time series could then be processed with pair-wise cross-correlation as before, to estimate the parameters of a wave model.

2 Methodology

The wavelet coherence of two TEC time series $T_1(t)$ and $T_2(t)$ is defined as

$$R^2_{1,2}(t,f) = \frac{\left|S(s^{-2}W_{1,2}(t,f)\right|^2}{S\left(s^{-1}\left|W_1(t,f)\right|^2\right) S\left(s^{-1}\left|W_2(t,f)\right|^2\right)} \tag{1}$$

where the cross-wavelet spectrum is $W_{1,2}(t,f) = W_1(t,f)W_2^*(t,f)$ and $S()$ is a smoothing operator. $W_x(a,b)$ is the complex-valued continuous wavelet transform (CWT) of $x(t)$

$$W_x(a,b) = \frac{1}{\sqrt{b}} \int_{-\infty}^{\infty} x(t)\psi\left(\frac{t-a}{b}\right) dt \tag{2}$$

in which ψ is a wavelet function, a is the scale, and b is the localized time index.

Strength of the wavelet coherence will indicate the presence, at time t, of signal structure at frequencies near f and can be used to design filters tuned to these individual components.

A tsunami was generated after the Peru earthquake on 23-June-2001 (20:33 GMT at 17.41^o S, 72.49^o W). This earthquake (M_w = 8.2) triggered a tsunami with local run-up reaching 2-5 m. The tsunami propagated across the Pacific Ocean, and was detected on tide gauge measurements along the coast of Japan. From the estimated arrival times (ETA) of the tsunami created by the Disaster Reduction and Human Renovation Institution (DRI) Japan, the tsunami propagated to the west coast of United States at 6:00-8:00 GMT on 24-June-2001. Ionospheric disturbances from this tsunami have been previously reported [1] through GPS measurements.

We used wavelet coherence analysis to detect the presence of ionospheric disturbances in dual-frequency GNSS time series collected by the GEONET (Japan) and SCIGN (Southern California) networks during this tsunami. Based upon the strength of the wavelet coherence, we were able to find two wave trains present in the data collected from both networks. These wave trains fell within frequency bands of approximately 1.6-5.5 mHz and 0.8-1.6 mHz. From these findings we applied filters, tuned to each band, to the TEC time series from every station in both networks. The two filtered time series were then independently processed by cross-correlation, is sub-areas of each network, estimating the speed and direction of each of the two disturbances within each of the sub-areas. The set of propagation speeds and directions were found to be compatible with a wave created by the tsunami. Propagation speeds of the two disturbances were estimated to be 630-661 m/s and 102-170 m/s, respectively. The propagation direction of both disturbances was compatible with the tsunami as the source. Speed of the lower-frequency disturbance was similar to that reported in [1] (150-200 m/s within a band of 0.5-5 mHz) and most likely was the result of an atmospheric gravity wave. Figure 3 shows the examples of the wavelet coherence for a pair of stations in the GEONET network, observing the same GPS satellite.

Figure 3 shows the propagation of the high-frequency disturbance over the GEONET network and the estimated propagation speed and direction from measurements from three satellites observed at the SCIGN.

3 General Conclusions

We have illustrated the use of wavelet methods for isolating coherent structure in the TEC time series from large networks of GNSS data and demonstrated these methods on data collected during the Peru tsunami of 23-June-2001. From this analysis, we have identified one disturbance most likely due to a gravity wave propagation from the Tsunami and another one at a higher propagation speed that could possible be an acoustic wave. Wavelet methods may offer a time-frequency analysis method for these disturbances, which could identify propagating disturbances in which the disturbance structure is time-varying or consists of multiple wave trains at different speeds and frequencies.

References

[1] J. Artru, V. Ducic, H. Kanamori, P. Lognonné, and M. Murakami. Ionospheric detection of gravity waves induced by tsunamis. *Geophysical Journal International*, 160(3):840–848, 2005.

[2] J.L. Garrison, S.C.G. Lee, J.S. Haase, and E. Calais. A method for detecting ionospheric disturbances and estimating their propagation speed and direction using a large GPS network. *Radio Sci*, 42, 2007.

[3] M. Hernández-Pajares, JM Juan, and J. Sanz. Medium-scale traveling ionospheric disturbances affecting GPS measurements: Spatial and temporal analysis. *J. Geophys. Res*, 111, 2006.

[4] Garrison J.L. Yang, Y-M and S-C Lee. Application of Wavelet Methods for the Detection and Analysis of Ionospheric Disturbances in GNSS Network Data. *Eos Trans. AGU, Fall Meet. Suppl*, 90(52), 2009. Abstract NH43C-1354.

[5] E. L. Afraimovich, N. P. Perevalova, and S. V. Voyeiko. Traveling wave packets of total elevtron content disturbances as deduced from global GPS network data. *Journal of Atmospheric and Solar-Terrestrial Physics*, 65:1245–1262, 2003.

[6] T. Dautermann, E. Calais, P. Lognonné, and G.S. Mattioli. Lithosphere-atmosphere-ionosphere coupling after the 2003 explosive eruption of the Soufriere Hills Volcano, Montserrat. *Geophysical Journal International*, 179(3):1537–1546, 2009.

[7] E. L. Afraimovich, K. S. Palamartchouk, and N. P. Perevalova. GPS radio interferometery of travelling ionospheric disturbances. *Journal of Atmospheric and Solar-Terrestrial Physics*, 60:1205–1223, 1998.

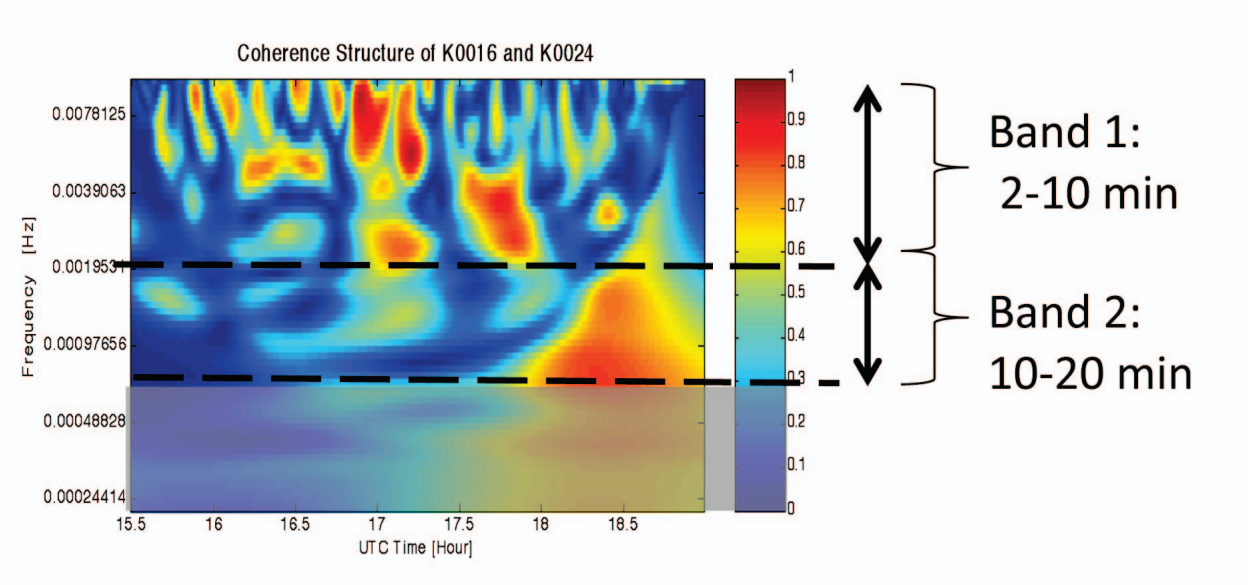

Figure 1: Example of wavelet coherence between GEONET Stations K0016 and K0024. Observe a high coherence in the 2-10 minute band persisting from approximately 16:00 to 18:00 H, followed by a second apparent disturbance in the 10-20 minute band starting at 18:00 H.

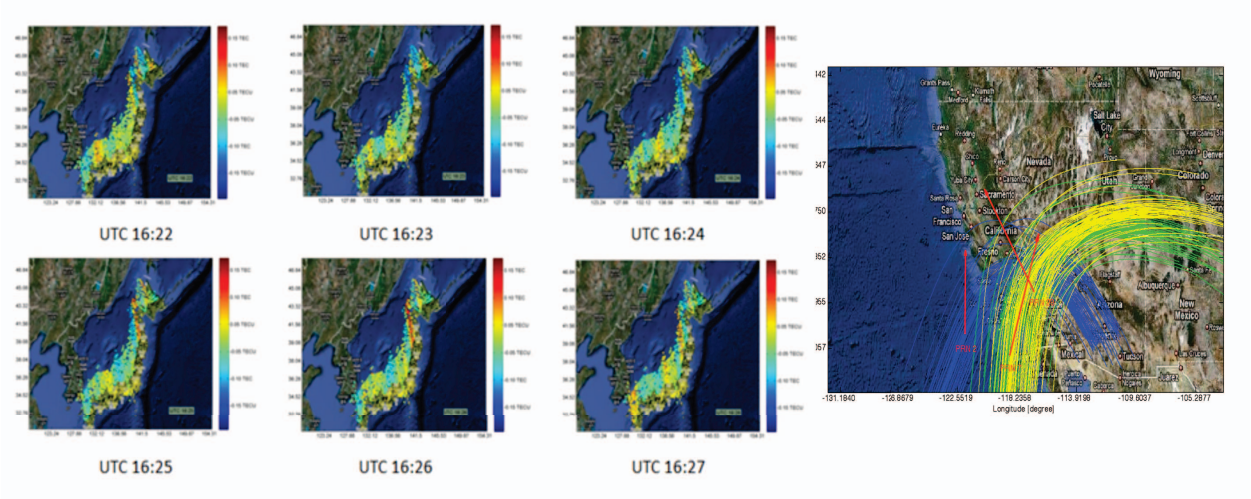

Figure 2: Left: Evolution of the disturbance over the GEONET network. Right: Estimation of the propagation speed and direction from satellites PRN 2, 7, and 28, indicated by the red vectors. Trajectories of the individual ionospheric pierce points from every station are shown, with the satellite indicated by the blue, yellow and green colors.